

Integrated Traffic Flow Based Optimization of Airport and Terminal Area

Ying HUO, Daniel DELAHAYE
OPTIM-Team/ENAC-LAB
ENAC – Université de Toulouse
Toulouse France

Ji MA
Civil Aviation University of China
CAUC
Tianjin China

Mohammed SBIHI
OPTIM-Team/ENAC-LAB
ENAC – Université de Toulouse
Toulouse France

Abstract—As air traffic demand exceeds available capacity, severe congestion during peak periods occurring at airports and the surrounding terminal airspace leads to flight delays as well as potential safety issues. This paper addresses the optimization problem of integrated traffic management of airport and terminal airspace on macroscopic level. Instead of evaluating the flight conflicts as we did in our previous research, a congestion evaluation model is proposed to quantify the flights for traffic flows in the terminal airspace and the runways, meanwhile, the occupancy evaluations of taxiway network and terminals are conducted. An adapted heuristic optimization method simulated annealing is implemented to solve the problem. Optimization process is put forward based on the case studies of Paris Charles De-Gaulle airport with 2.5-hour data. The comparisons between initial traffic data and optimized solution are provided and the advantage of the proposed model is analyzed. In the aspect of time uncertainty, simulations based on the proposed model and the model of our previous work are conducted, the final results indicate that our model shows an advantage in uncertainty absorption over the previous work.

Keywords—Integrated Optimization, Terminal Maneuvering Area, Airport, Simulated Annealing

I. INTRODUCTION

As air traffic congestion increases, air traffic delays become more and more severe. The frequent communication all over the world urges the development of air transportation. The imbalance between demand and available resources of air transport causes a significant growth in delay, which increases air traffic service dissatisfaction and economic loss. Airport and its surrounding airspace are considered as a very complex region, thus the study of air traffic flow management (ATFM) concentrated in airport and Terminal Maneuvering Area (TMA) needs technical operation strategies and fully analytical evaluations.

Due to the distinct and complex characteristics of terminal airspace and airport, segregated researches have been studied widely. Murça *et al.* [1] studied the flight scheduling problem in the terminal area by considering the dynamic characteristic of flights in the airspace and the benefits of alternative routes. In [2–4], runway scheduling and taxiway scheduling were studied to enhance the coordination of the integrated airport management.

Although airport and TMA are usually considered as two individual areas due to their different configurations, the fact that airport and its surrounding airspace have a direct and

interacted connection attracts considerable interests towards the integrated research of terminal area and airport including integration of arrival management, departure management and surface management. The integrated research related sub-problems of routing, sequencing and conflict resolutions are investigated as well [5, 6].

Though there are lots of researches focusing on the microscopic level, the real-time management of airport and flight operations still rely on the decisions of air traffic controllers who provide feasible flight instructions according to operating rules and personal experience. Considering this situation, our study addresses the problem in a macroscopic perspective and tries to provide a solution for the integrated airport and terminal management without considering the specific instructions from the controllers.

In our previous work [7], the integrated problem of terminal airspace management and airport management on a macroscopic level was studied, however, the presented evaluation model took microscopic metrics of flight by flight conflicts into consideration. On macroscopic level, air traffic should be considered in a larger scale, while the investigation of detailed flight interactions are easily effected by minor uncertainty that generated during the flight operation. In order to emphasize the congestion elimination and robustness at the same time, traffic flow-based approach is proposed. The objective of our study is to mitigate the congestion and conflict resolution workloads in the terminal area and reduce the overload of each element in the airport. The proposed model focuses on the density of traffic flow which is less sensitive in terms of time variation comparing to the model in our previous work.

The paper is organized as follows: section II provides an overview of the proposed network abstraction. The mathematical problem is clarified, the evaluation method is described as well. Section III displays the case study based on real data of Paris-CDG airport. In section IV, optimization results are analyzed, and the results of the simulations regarding time uncertainty are displayed. Section V concludes the whole paper.

II. MATHEMATICAL MODELING

Our model is developed to contribute to both arrival and departure flights optimization in the airport and its surrounding airspace. A network abstraction is established to centralize the

optimization process on network resources. The resources in the system are TMA routes, runways, taxiway network and terminals. With the proposed method, flight movements are grouped and quantified by time intervals.

A. Network model of TMA and airport surface

In the TMA, the route network is represented by links and nodes. The node-link structure can be presented as graph $(\mathcal{N}, \mathcal{L})$, where \mathcal{N} is the node set and \mathcal{L} is the link set. We have $\mathcal{N} = N_e \cup N_w \cup \{r\}$ that constitutes the route network, where $N_e = \{\text{MOPAR}, \text{LORNI}, \text{OKIPA}, \text{BANOX}\}$ represents the set of entering points of the TMA, r represents the node at the runway threshold, and $N_w = \{n_e^2, \dots, n_e^{r-1}\}$ is the set of nodes between the entry point e and the runway threshold. Similarly, we have $\mathcal{L} = L_e \cup L_w \cup \{l_r\}$, where $L_e = \{1, \dots, l_e\}$ is the set of links that connects the entry nodes, l_r is the last link of the route connecting runway threshold, L_w is the set of remaining links. Each entry point $e \in N_e$ corresponds to one route that is defined by $r_e = \{e, l_e^1, n_e^2, l_e^2, \dots, n_e^{r-1}, l_r, r\}$ in the airspace with a slight change at the last node due to different runway assignment. Each route is defined by a succession of nodes and links, flights follow one of these routes according to their entry points and landing runways.

Fig. 1 shows the arrival route network abstraction of Paris Charles-De-Gaulle (CDG). One of the arrival routes from OKIPA to runway 26L is marked and relevant notations are displayed. We consider the links that converge to one node as the parent links of this node. In our network, we have $|\mathcal{N}| = 15$ nodes and $|\mathcal{L}| = 15$ links.

Three main resources in the airport are considered: runways, taxiway network and terminals. Each of the components will be considered as a resource with a certain capacity or relevant congestion constraints, the network resources are generally represented as $\mathcal{S} = \mathcal{N} \cup \mathcal{L} \cup \mathcal{R} \cup \mathcal{T}_e \cup t_a$, where \mathcal{R} and \mathcal{T}_e denote runway sets and terminals respectively. t_a represents the taxi network.

B. Notations

Assuming that we are given a set of flights $\mathcal{F} = \{1, \dots, F\}$, among them, three types of flight operations are included, $\mathcal{F} = \mathcal{A} \cup \mathcal{D} \cup \mathcal{AD}$, where \mathcal{A} stands for arrival, \mathcal{D} stands for departure and \mathcal{AD} represents connected flights.

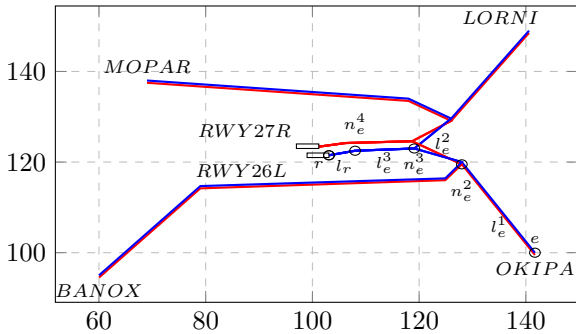


Figure 1. Arrival route structure

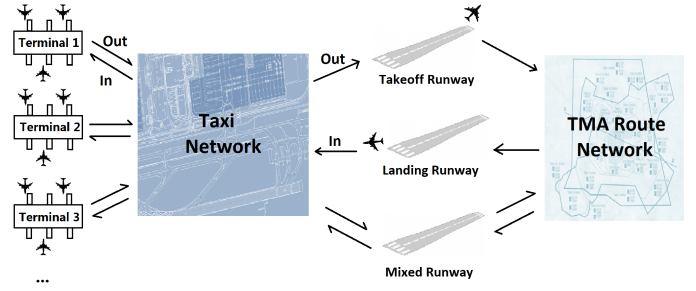


Figure 2. Network model of TMA and airport surface

Different flight information are given regarding the flight types.

- C_f : Wake turbulence category ($f \in \mathcal{F}$).
- M_f : Assigned terminal ($f \in \mathcal{F}$).
- E_f : Entry node of the TMA ($f \in \mathcal{A} \cup \mathcal{AD}$).
- T_f^o : Initial RTA (Required Time of Arrival) of entering the TMA through the entry node ($f \in \mathcal{A} \cup \mathcal{AD}$).
- V_f^o : Initial speed of entering the TMA through the entry node ($f \in \mathcal{A} \cup \mathcal{AD}$).
- R_f^o : Initial assigned landing runway ($f \in \mathcal{A} \cup \mathcal{AD}$).
- t_f^{ad} : Turn around duration ($f \in \mathcal{AD}$).
- T_f^d : Scheduled off block time ($f \in \mathcal{D}$).
- R_f^d : Initial assigned departure runway ($f \in \mathcal{AD} \cup \mathcal{D}$).

The common information of all flights are C_f and M_f . For arrival flights, the information of E_f , T_f^o , V_f^o , R_f^o are given. For departure flights, T_f^d and R_f^d are provided and for connected flights, except the information of arrival and departure flights, an additional data of t_f^{ad} is accessible.

The exact time at which a flight arrives at a resource can be calculated with some assumptions:

- In TMA, we assume that the speed of flights will constantly decelerate until the Final Approach Fix (FAF) and then keep constant till the threshold of the runways. Final speeds for arriving at runways are set as 110 kt 130 kt and 150 kt for small, medium and large aircraft respectively.
- The runway occupation time is obtained from the flight operation standards regarding the flight category.
- The taxi duration is measured empirically. According to the airport operation information, the average taxi time for each flight can be obtained with regard to the combination of terminal and runway. Tab. I and Tab. II show the taxi-in and taxi-out time that we use in this paper.
- The in-block time for each arrival flight can be obtained

TABLE I
AVERAGE TAXI-IN DURATION BETWEEN RUNWAY AND TERMINAL (IN SECONDS)

Landing runway	Terminal 1	Terminal 2	Terminal 3
27R	400	730	680
26L	535	500	530

TABLE II
AVERAGE TAXI-OUT DURATION BETWEEN TERMINAL AND RUNWAY(IN
SECOND)

Departure runway	Terminal 1	Terminal 2	Terminal 3
27L	720	890	880
26R	1400	760	710

by adding the runway occupancy time and average taxi-in duration to the real landing time.

- For the departure flights, the evaluation is conducted until the take-off segment, the take-off time is estimated by adding up the taxi-out duration and the off-block time.
- The take-off time of a connected flight can be computed by using the in-block time plus the turn around duration and average taxi-out time.

By using the flight operation standards, we can obtain the runway occupancy time. Along with the given information, the operation time frame of all flights can be gathered.

C. Decision variables and constraints

The optimization model that we propose contains four types of decision variables: TMA entry time, TMA entry speed, landing runway and push back delay. The associated parameters are selected and interpreted as follows:

1) *Entry time*: in the TMA, flights ($f \in \mathcal{A} \cup \mathcal{AD}$) can adjust the time to enter the TMA by changing the en-route speed. Discrete time is used and ΔT which denotes the time slot is considered as one unit to measure the total time range. The maximum tardiness and earliness are represented as ΔT_{max} and ΔT_{min} . The possible time range for each decision variable is composed of multiple ΔT . Therefore, for each flight ($f \in \mathcal{A} \cup \mathcal{AD}$), a decision variable $t_f \in \mathcal{T}_f$ has a flexible range of: $\mathcal{T}_f = \{T_f^o + j\Delta T | \Delta T_{min}/\Delta T \leq j \leq \Delta T_{max}/\Delta T, j \in \mathbb{Z}\}$, where j denotes the interest of time slot deviation from the initial arrival time. Considering the flight operations in reality, the entry time range is set as $\Delta T_{max} = 30 \text{ min}$ and $\Delta T_{min} = -5 \text{ min}$.

2) *Entry speed*: We discretize the entry speed in an similar way as the entry time. For flights $f \in \mathcal{A} \cup \mathcal{AD}$, an entry speed decision variable $v_f \in \mathcal{V}_f$ has a constraint of:

$$\mathcal{V}_f = \{V_f^{min} + j\Delta_f^v | 0 \leq j \leq (V_f^{max} - V_f^{min})/\Delta_f^v, j \in \mathbb{N}\}.$$

In this study, we set $V_f^{min} = 0.9V_f^o$, $V_f^{max} = 1.1V_f^o$ and $\Delta_f^v = 0.01V_f^o$. We also guarantee a prior requirement that V_f^{max} do not exceed the maximum speed limited by the aircraft type.

3) *Runway assignment*: For $f \in \mathcal{A} \cup \mathcal{AD}$, landing runway assignment decisions are represented by $r_f^a \in \mathcal{R}_f^a$. Two landing runways are dedicated to arrival flights to balance the capacity of runways during the peak hours of operation. Departure runway assignment is not included in our research.

4) *Pushback delay*: For $f \in \mathcal{D} \cup \mathcal{AD}$, it has been verified that the delay on the ground has more economic benefits than in the air. Therefore, pushback delay rather than air delay is considered as decision variable $p_f \in \mathcal{P}_f$:

$$\mathcal{P}_f = \{P_f^o + j\Delta T | 0 \leq j \leq \Delta T_{max}^p/\Delta T, j \in \mathbb{N}\},$$

where ΔT_{max}^p denotes the maximum allowed delay time. In our case, the maximum delay is chosen to be 20 min which is a reasonable time range in practice.

To summarize, the decision variables associated to flight f denoted as x_f .

$$x_f = (t_f, v_f, r_f^a, p_f)$$

Let's denote $\mathbf{x} = (x_1, \dots, x_F)$ as a set of decision variables of all flights.

D. Objective

Our models are designed to eliminate the conflict resolution workload in the air and alleviate congestion in the whole system. The resources in this study are evaluated separately and the objective function is thus a weighted sum of evaluation metrics of five resources:

$$\min \sum_{s \in \mathcal{S}} \gamma_s \cdot G_s(\mathbf{x}), \quad (1)$$

where γ_s is a user-defined weighting coefficient for the congestion or exceeded overload of resource s in the model system. $G_s(\mathbf{x})$ is the corresponding objective for each resource s .

The objective is evaluated by two metrics, the first one can be interpreted as the average congestion during time horizon T which is the mean capacity exceeding value for all evaluation in time horizon. Another important metric measures the maximum overload, which is the difference between the maximum overload and the corresponding capacity. Mean congestion provides a general perspective of network situation in terms of flight numbers, and the maximum overload indicates the period at which severe congestion occurs. A general objective function G without evaluation details is formulated as follows:

$$G(\mathbf{x}) = \sum_{s \in \mathcal{S}} \gamma_s \left[\frac{1}{T} \sum_{t \in T} [\max(E_s(t) - C_s, 0) \cdot \Delta] \right] + \sum_{s \in \mathcal{S}} \gamma_s \left[\max_{t \in T} [\max(E_s(t) - C_s, 0)] \right], \quad (2)$$

where $E_s(t)$ represents the evaluation result of resource s at the evaluation time indicated by t , and C_s indicate the resource capacity. We define E_s to be the flight number distribution for resource s along T . Δ is a time unit for the discrete time horizon.

Once the decision variables are set, we can calculate the time when aircraft arrive at each resource. Then we use the desired time values to compute E_s . Considering the different characteristics of each resource, the evaluation of E_s need to be specified. Evaluation process is introduced in the following section.

E. Traffic flow-based evaluation

Traffic flow-based approach is implemented on the operated traffic flow which is a series of scheduled flights specified with operation time. We investigate the traffic flow by focusing on specific time intervals. For each time interval, the number of flight that entry or exit the network resources are counted.

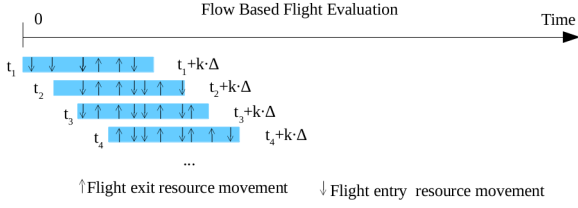


Figure 3. Traffic flow-based evaluation

In order to detail the evaluation and enhance the accuracy of our model without a huge loss of the flight information, a series of evaluations are conducted based on a fixed time period, for each evaluation, the starting time is shifted by one time step.

In the process of traffic flow-based evaluation, Δ (e.g. 1 minute) is set as a time unit that constitutes the evaluation time interval and as a time step to proceed to the evaluation process. According to different attributes on each resource, the evaluation time interval $L = k \cdot \Delta$ should be set differently where k is a coefficient to define the length of the evaluation time.

Fig. 3 illustrates the evaluation time scheme based on the traffic flow-based approach. The blue strips indicate a time interval of L for each evaluation in which the number of flights that entry or exit a specific resource are counted. A continuous moving of the evaluation time is proceeded by shifting one time step afterward.

1) *Link*: The preliminary evaluation for link is the number of flights that enters a link. With the utilization of traffic flow-based approach, the evaluation time interval should be decided. Considering that a short evaluation time interval is not able to reflect the flight density and can not achieve a proper comparison with link capacity, thus $k = 10$ is used to define the link evaluation time.

For the link evaluation, the number of flights that enters link l from t to $t + L$ is evaluated as follows:

$$E_l(t) = \sum_{i=t}^{t+L} \sum_{f \in \mathcal{F}} \omega_{l,f}^i \quad l \in \mathcal{L}, \quad (3)$$

where $\omega_{l,f}^i$ is a binary parameter that equals to 1 if flight f is supposed to enter the link l during time interval i to $i + L$, otherwise equals to 0.

Based on the aforementioned assumption, flights are conducted with a constant deceleration procedure which begin from the entry point of TMA until the FAF. Regarding the different spatial locations of links, flight speeds are distributed differently on each link, so the average speed v_l of all passed flights on link l is estimated. Along with the flight separation requirements, the acceptable number of flights that enters link l during the evaluation period can be obtained and set as a capacity of link l for the following congestion evaluation.

The number of flights on each link in the TMA is constrained by $M = 1$ flight per 5NM which is derived from the

flight operation rules. Based on the average speed of each link, the associated link capacity C_l can be computed as:

$$C_l = \frac{M \cdot v_l}{K} \quad (4)$$

where K is a time scale. As in link, k equals to 10, Δ is fixed to be one minute and the unit of link average speed is NM/h, $K = 1 \text{ hour}/L$ is a scale to convert the flight entry number of a specific link of 1 hour into a time of 10 minutes.

2) *Node*: In the TMA, nodes evaluation is focused on the estimation of potential conflicts resolution workload. Using the evaluation model proposed in [8], the quantification of conflicts resolution workload is determined by two converging traffic flows which perfectly match the scenario of nodes and their parent links. Suppose that two links l_i and l_j are parent links of node n , flight speed on the links are given as v_{l_i} and v_{l_j} respectively. $E_{l_i}^{out}$ and $E_{l_j}^{out}$ are the distributions of number of flights that exit the parent links during the time horizon, thus the conflicts resolution workload $E_n(t)$ on a specific time interval indicated by t can be computed as follows:

$$E_n(t) = \frac{2N_s \sqrt{v_{l_i}^2 - 2v_{l_i}v_{l_j} \cos \theta_{ij} + v_{l_j}^2}}{v_{l_i}v_{l_j} \sin \theta_{ij}} \cdot E_{l_i}^{out}(t)E_{l_j}^{out}(t) n \in \mathcal{N}, \quad (5)$$

where N_s is a parameter for the standard separation norm, θ_{ij} denotes the angle formed by two convergent flows associated with link l_i and l_j .

For nodes, the conflict resolution workload is set to be 6 per hour regarding the workload of air traffic controller.

3) *Landing runway*: Runway flight evaluation counts the number of flights that pass through the runway threshold from time t to time $t + L$, where $k = 10$ ($L = k \cdot \Delta$) ensures an adequate time interval for avoiding the potential risk of losing flight information. Along with the time going, flight entry distribution E_r of the whole time horizon regarding arrival runway is formulated as Eq. 6 and the runway operation limitation can be imposed to calculate the sub-objective generated by runway.

$$E_r(t) = \sum_{i=t}^{t+L} \sum_{f \in \mathcal{F}} \omega_{r,f}^i \quad r \in \mathcal{R}, \quad (6)$$

same as in Eq. 3, $\omega_{r,f}^i$ is a binary parameter to indicate that flight f uses runway r during time interval i to $i + L$ and equals to 0 otherwise.

4) *Taxiway network and terminal*: Taxiway network and terminal are resources with specific capacities. We can verify whether the number of flights exceeds the capacity or not at any time, therefore the congestion evaluation is conducted on each time step with a time interval of $L = \Delta$. In this case, there is no overlap of evaluation time, evaluation intervals are separated and continuous. Flights that enter and exit the resource are recorded at each time interval to evaluate the number of flights that stay on terminal or taxiway network during time t to $t + L$.

$$E_{t_a}(t) = \left(\sum_{f \in \mathcal{F}} \omega_{t_a, f}^t - \sum_{f \in \mathcal{F}} \delta_{t_a, f}^t \right) + Q_{t_a} \quad (7)$$

Eq. 7 takes taxiway as example. $\omega_{t_a, f}^t$ is an mentioned binary parameter for taxiway. $\delta_{t_a, f}^t$ is also a binary parameter that equals to 1 if flight f is supposed to proceed an exit operation of taxiway during time t to $t + L$ and otherwise equals to 0. Q_{t_a} denotes the initial number of flights that stay in the taxi network at the time that we start the current evaluation. The evaluation process of terminals is the same as in the taxiway network. Based on flight number distribution, the two objective metrics regarding the specific resources can be computed.

III. SOLUTION APPROACH

It is known the computation for this problem is very expensive and NP-hard [9]. If we consider $|\mathcal{A}| + |\mathcal{AD}| + |\mathcal{D}|$ flights with the entry time changes $|\mathcal{T}_f|$, entry speed changes $|\mathcal{V}_f|$, landing runways $|\mathcal{R}_f|$ and pushback delay changes $|\mathcal{P}_f|$, the total number of possible combinations of decision variables is equal to $(|\mathcal{T}_f| \cdot |\mathcal{V}_f| \cdot |\mathcal{R}_f| \cdot |\mathcal{P}_f|)^{|\mathcal{AD}|} + (|\mathcal{T}_f| \cdot |\mathcal{V}_f| \cdot |\mathcal{R}_f|)^{|\mathcal{A}|} + |\mathcal{P}_f|^{|\mathcal{D}|}$. Considering an example of 100 flights containing 25 arrival flights, 50 connected flights and 25 departure flights. In this example, we assume that $|\mathcal{T}_f| = 400$, $|\mathcal{V}_f| = 20$, $|\mathcal{R}_f| = 2$ and $|\mathcal{P}_f| = 200$, then there would be a huge possible solutions to be considered. Due to this high combinatorics, simulated annealing algorithm is put forward to address the problem.

A. Simulated annealing

Simulated annealing is a meta-heuristic algorithm to approximate global optimization in a large search space for an optimization problem. It is used to find an approximate global optimum other than a precise local one in a fixed amount of time. This approach is interpreted as a slow decrease in the probability of accepting worse solutions as the solution space is explored. At each time step, the algorithm selects a solution close to the current one noted as its neighborhood solution, the quality of this solution is measured, and the decision is made to move to it or to stay with the current solution based on the fact that the new solution is better or worse than the current one. With this procedure repeating, the approximate global optimum solution can be achieved [10].

In our case, in order to mitigate computational burden, a *performance indicator* is introduced to increase the probability of finding a better neighborhood solution. During the evaluation, flights who have a chance to violate the capacity constraint in any resource are marked with the overload. Total performance indicator is represented as m_f for flight f which is the sum of exceeded capacity that flight f has experienced in the network. That is to say, if on a specific resource s , $E_s(t)$ exceeds the capacity at evaluation time interval t , and flight f is one of the flights that contributes to this overload, then this overload will be considered as a part of performance indicator and added to m_f .

In our algorithm, indicators are categorized into airspace performance a_f and ground performance g_f according to

Algorithm 1 Neighborhood solution selecting method

Require: For each flight, compute a_f and g_f and $m_f = a_f + g_f$, generate a random number $n = \text{random}(0,1)$;
 $p_a^f = a_f / m_f$;
 $p_g^f = g_f / m_f$;
1: Choose one flight f based on its total performance;
2: **if** $f \in \mathcal{A}$ **then**
3: **if** $n < p_a^f$ **then**
4: one of t_f, v_f is chosen with equal probability and change its value.
5: **else**
6: one of t_f, v_f and r_f^a is chosen with equal probability and change its value.
7: **end if**
8: **else if** $f \in \mathcal{D}$ **then**
9: change \mathcal{P}_f
10: **else if** $f \in \mathcal{A} \cup \mathcal{D}$ **then**
11: **if** $n < p_a^f$ **then**
12: one of t_f, v_f is chosen with equal probability and change its value.
13: **else**
14: one of t_f, v_f, r_f^a and p_f is chosen with equal probability and change its value.
15: **end if**
16: **end if**

the location of the constraints violation. The values of sub-performance decide the selection of decision variable due to a fact that for a flight which encounters an airspace overload is useless to change the value of pushback delay. The designed algorithm considers all the marked flights. One of them will be chosen and assigned a new value for the picked decision vari-

Algorithm 2 Simulated annealing application

Require: Initialize(initial temperature T_0 , iteration $I = 200$, random number $\beta \in [0, 1]$);
1: Calculate the initial sequence objective $s(\mathbf{x})$;
2: $s_b(\mathbf{x}) \leftarrow s(\mathbf{x})$
3: **while** $T_c > 0.0001 \cdot T_0$, $s_b(\mathbf{x})$ is not optimum solution **do**
4: **for** $i = 1$ to I **do**
5: Choosing and changing the decision variable of flight f as neighborhood according to neighborhood selecting rules;
6: Calculate the new objective $s_i(\mathbf{x})$;
7: **if** $s_b(\mathbf{x}) > s_i(\mathbf{x})$ **then**
8: $s_b(\mathbf{x}) \leftarrow s_i(\mathbf{x})$;
9: **else if** $\beta < \exp\left(\frac{s_i(\mathbf{x}) - s_b(\mathbf{x})}{T_c}\right)$ **then**
10: $s_b(\mathbf{x}) \leftarrow s_i(\mathbf{x})$;
11: **end if**
12: **end for**
13: $T_c = T_c \cdot 0.99$;
14: **end while**
15: **return** $s_b(\mathbf{x})$

TABLE III
AIRPORT COMPONENTS CAPACITY

Landing Runway	Departure Runway	Terminal 1	Terminal 2	Terminal 3	Taxiway
30/h	40/h	20	130	25	19

able so as to generate the neighborhood solution. Algorithm 1 describes the procedure to find the neighborhood solution. The change of decision variable is the change of time deviation or speed deviation corresponding to the initial value with a range stated in the explanation for decision variables. Algorithm 2 presents the implementation of simulated annealing with the consideration of Algorithm 1 in which T_c denotes the current temperature of the optimization process and $s_b(\mathbf{x})$ is the obtained best solution considering all the finished iteration.

IV. RESULTS

A. Case study background

The instances that we used in this paper are the real scheduling data of Paris CDG airport. In this airport, there are two runway configurations: West-flow (26L, 27R—26R, 27L) and East-flow (09L, 08R—09R, 08L). This paper focuses on the more frequently used West-flow configuration. The airport consists of three terminals, in which terminal 2 handles the most amount of flights.

The congestion evaluation standard of the related capacity of each component will be chosen according to the flight regulation and empirical estimation. The capacities of resources in the airport are estimated by using historical data which is shown in Tab. III. We would like to mention that in the taxiway, the acceptable number of flights is fluctuating due to different flight types, speeds or taxiway changing in practice. Thus the capacity of taxiway is confirmed during the process of problem solving by giving other resources priority. Then we choose the lowest flight accumulation in the taxi network as the taxiway capacity.

Actual flight data on 18th February 2016 from 7:00 AM to nearly 9:40 AM which was the peak hour of the day are studied in this work. Flights are mostly composed of heavy and medium types with a mix ratio of *Heavy* : *Medium* = 23% : 77%. The model was coded in Java and run on a 2.50GHz core i7 CPU, under Linux operating system. The required time for computation is around 5 minutes.

The resources in the network system are evaluated separately with different capacities, thus the respective analysis is made for each resource set.

B. Results analysis

1) *Link*: Regarding the network abstraction, the link number is counted up to 15, by analyzing the initial flight data, only six of them experience congestion. Two of them are displayed as examples. In Fig. 5, blue lines represent the original scheduling data derived evaluation distributions and the red lines are the optimized results obtained by heuristic

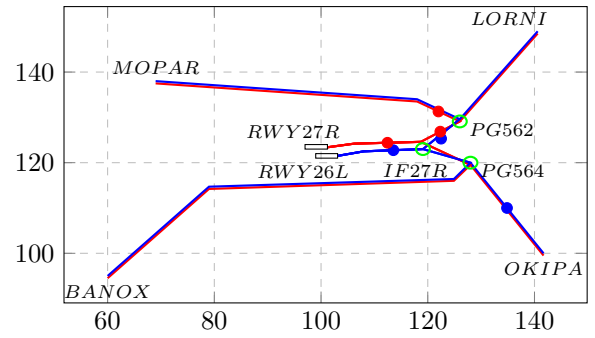


Figure 4. Network congestion indication

method. The x -axis indicates the start time of each evaluation which is aforementioned as t . Other links are solved with same process and similar results are achieved. Fig. 4 uses red and blue points in the middle of the links to indicate the initial congested links. Note that the average speed on each link are different based on Eq.4, the imposed capacities marked in Fig. 5 are different.

2) *Node*: Since the evaluation time interval is set as 10 minutes, for each interval, the obtained data is finally transferred to an hour. As the conflicts calculation is highly related to the number of flights coming from the parent links, thus for some nodes, no overload is appeared during the evaluation time, but still, there are three nodes who have overloads from the initial scheduling data. Fig. 4 displays nodes that have their capacity exceeded with initial flight data are marked with the green circles.

Fig. 6 displays the comparison of conflicts resolution workload distributions before and after optimization, the indicated quantities of the red lines show that hourly conflicts resolution workloads are reduced to the required standard.

3) *Runway*: In each runway, similar evaluation process is conducted as in link. The flight number distributions are compared directly. From Fig. 7, we can see that the red

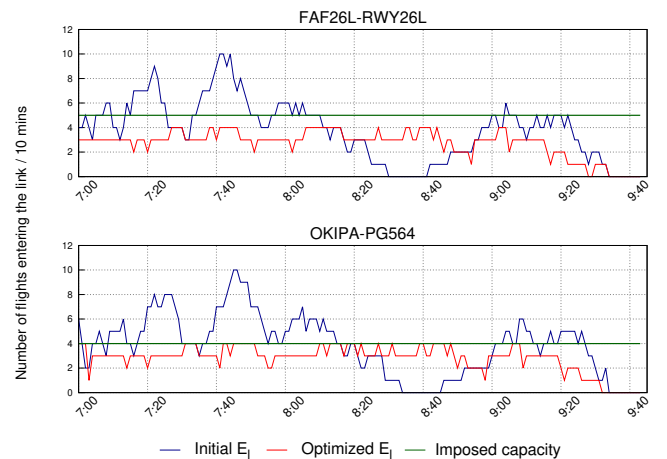


Figure 5. Comparison of link occupancy

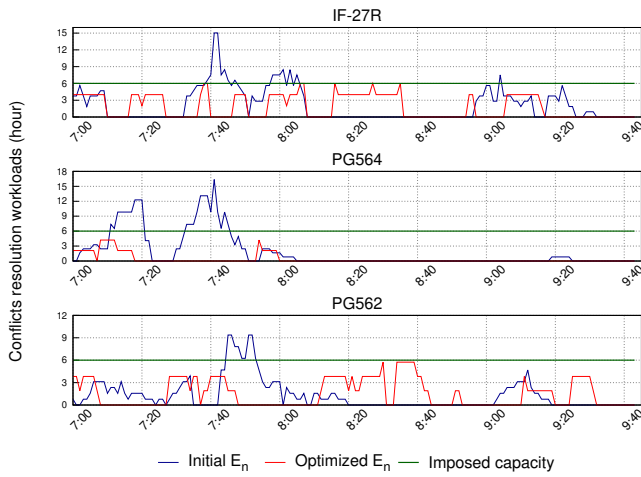


Figure 6. Conflicts resolution workload comparison on nodes

lines which indicate the optimized flight number distributions become smoother after the optimization. Since runway 27R and 26L are arrival runways, the traffic peaks of landing runway 27L and 26R are different. After optimization, the flight distributions totally satisfy the capacity constraint requirements.

4) *Taxiway*: In Fig. 8, the blue line is the initial flight distribution on taxiway with respect of time which shows large fluctuation. The capacity setting is done in the process of optimization considering the performances of other resources. As shown in the red line, the occupancy of the taxiway can be effectively reduced with a smoother distribution which will provide a much safer environment during the operation of flights.

5) *Terminal*: Due to the airport configuration, although terminal 2 has most of the flight gates, it is the busiest terminal and easy to generate a congestion. Fig. 9 shows the comparison between initial gate occupancy distribution and the one after optimization. The capacity is set to be 130, while

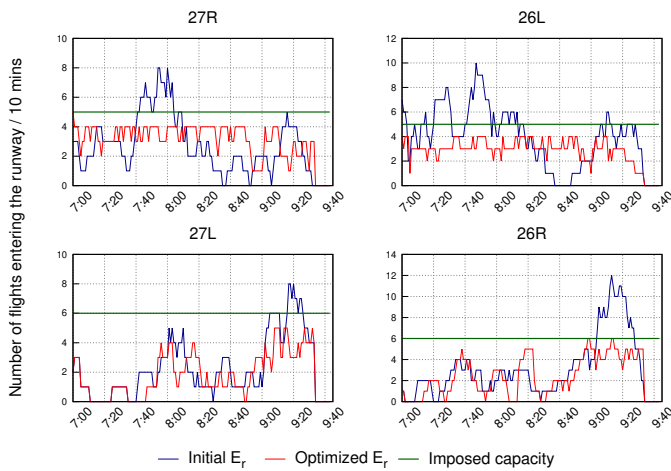


Figure 7. Comparison of runway occupancy

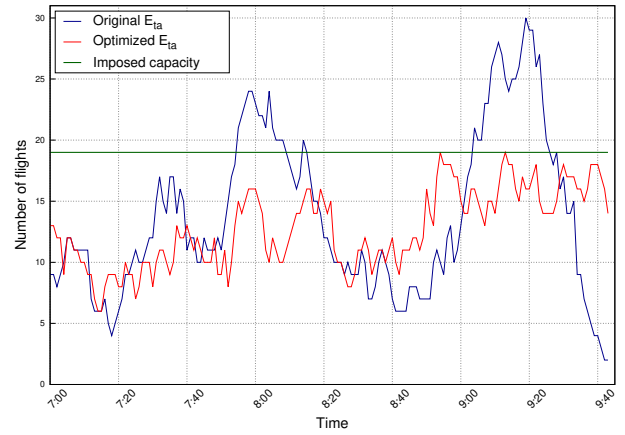


Figure 8. Comparison of taxiway network occupancy

after optimization, the maximum gate occupancy becomes 124. The flight distribution perform a tendency to manipulate the flights from the peak hour to an idle time period so as to ensure safety and make better use of the resources.

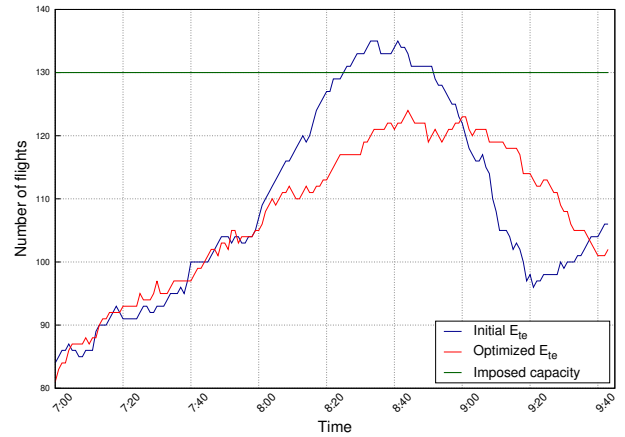


Figure 9. Initial and optimized gate occupancy comparison of terminal 2

C. Robustness simulation

As a model focus on traffic flow evolution and evaluate a series of flight status at the same time, the advantage of uncertainty resistance can be found. Thus a simulation is conducted with an reference case of our previous study. The optimal solutions of traffic flow-based model and flight by flight conflict evaluation model which is proposed in [7] are obtained with the same input data. since the two models have different targets and distinctive perspectives, the robustness tests are conducted respectively with their own optimal solutions with respect to their own objective. In each simulation, random perturbations are drawn from uniform distribution of $[-\varepsilon, \varepsilon]$ for three different values of ε . Each simulation has 5000 experiments and the average values of objective and sub-objectives of each model are obtained and displayed in Tab. IV. For the two models, the sub-objective of airside evaluations are the same. In TMA, flight by flight conflict evaluation model

TABLE IV
ROBUSTNESS TEST RESULTS OF TWO MODELS WITH THREE KINDS OF PERTURBATION.

Average congestion/conflicts	Traffic flow-based model				Flight by flight conflict evaluation model			
	Perturbations according to uniform distribution on $[-\varepsilon, \varepsilon]$							
	Initial congestion	$\varepsilon=0.5\text{min}$	$\varepsilon=1\text{min}$	$\varepsilon=2\text{mins}$	Initial conflict	$\varepsilon=0.5\text{min}$	$\varepsilon=1\text{min}$	$\varepsilon=2\text{min}$
Node	0	6.585	10.1	16.56	0	21.07	44.882	78.37
Link	0	0.474	0.963	1.62	0	4.94	43.975	144.55
Runway	0	0	0.064	0.47	0	14.998	31.05	52.86
Taxiway	0	0	0.00134	0.033	0	0.519	0.596	0.835
Terminal	0	0	0	0	0	0	0	0
Sum	0	7.06	11.136	18.69	0	41.54	120.5	276.6

computes the conflicts generated on each resource, while the proposed model take the average congestion and maximum overload into account.

Two parts in the table are highlighted: the simulation results for the traffic flow-based model and for the flight by flight model. For each model, as the range of perturbation increased, the derived congestion or conflicts augment. One exception is revealed due to the inherent attributes that terminal is a resource with specific capacity and the small perturbations have minor effects on the number of flights in terminals. As we compare the result of two models with the same perturbation, regardless the values of the results or the growth rates, traffic flow-based model has a better performance than flight by flight conflict evaluation model. The results indicate that flight by flight conflict evaluation model is very sensitive to the time variation yet traffic flow-based model shows a strong resilience in the face of uncertainty.

V. CONCLUSION

This work contributes to the terminal and airside integrated flight scheduling problem in a macroscopic perspective. Based on the past deterministic work, new considerations are included in the research for each network resource. The goal of this work is to reduce the congestion and controller intervention workload in the terminal area and the overload in the airport.

In this paper, network abstraction is proposed based on the distinctive characteristics of different resources so as to conduct separated investigation on each kind of resource. In order to mitigate the congestion in the network as well as increase the stability against time variation, traffic flow-based approach is put forward. In TMA as well as runway, flights are grouped and counted in a specific time interval, corresponding capacity is set so as to ensure the general safety and separation. In airside, the taxiway and terminal congestion are considered. An heuristic method of simulated annealing is proposed to solve the optimization problem. Practical instances of Paris CDG airport are used. Promising results are demonstrated in detail in terms of each resource. For verifying the model, a robustness test towards the proposed model and the model in our previous work is conducted, the results indicated that the traffic flow-based model is less sensitive than the other one.

As for future works, multiple airports system contains more uncertainties which yields a complex and imprecise study on microscopic level, thus the further research could be dedicated to a larger range of research of including other airports in the system.

ACKNOWLEDGEMENT

This work has been supported by China Scholarship Council (CSC). The author is gratefully acknowledge the support of Mr. Serge Roux for his assistance with technical improvements.

REFERENCES

- [1] M. C. R. Murça and C. Müller, "Control-based optimization approach for aircraft scheduling in a terminal area with alternative arrival routes," *Transportation research part E: logistics and transportation review*, vol. 73, pp. 96–113, 2015.
- [2] R. Deau, J.-B. Gotteland, and N. Durand, "Airport surface management and runways scheduling," 2009.
- [3] D. Kjenstad, C. Mannino, P. Schittekat, and M. Smedsrud, "Integrated surface and departure management at airports by optimization," in *2013 5th International Conference on Modeling, Simulation and Applied Optimization (ICMSAO)*, pp. 1–5, IEEE, 2013.
- [4] H. Balakrishnan and Y. Jung, "A framework for coordinated surface operations planning at dallas-fort worth international airport," in *AIAA Guidance, Navigation and Control Conference and Exhibit*, p. 6553, 2007.
- [5] D. Kjenstad, C. Mannino, T. E. Nordlander, P. Schittekat, and M. Smedsrud, "Optimizing aman-smam-dman at hamburg and arlanda airport," *Proceedings of the SID, Stockholm*, 2013.
- [6] G. Pavese, M. Bruglieri, A. Rolando, and R. Careri, "Dman-smam-aman optimisation at milano linate airport," *Eighth SESAR Innovation Days*, 2017.
- [7] J. Ma, D. Delahaye, M. Sbihi, and M. Mongeau, "Integrated optimization of terminal manoeuvring area and airport," in *6th SESAR Innovation Days (2016)*, pp. ISSN-0770, 2016.
- [8] D. Delahaye and S. Puechmorel, *Modeling and optimization of air traffic*. Wiley Online Library, 2013.
- [9] J. E. Beasley, M. Krishnamoorthy, Y. M. Sharaiha, and D. Abramson, "Scheduling aircraft landings: the static case," *Transportation science*, vol. 34, no. 2, pp. 180–197, 2000.
- [10] E. Aarts and J. Korst, "Simulated annealing and boltzmann machines," 1988.